PAPER

Check for updates

Synthesis of heat storage ceramic λ-Ti₃O₅ using titanium chloride as the starting material†

Tomoko Kubota,[a] Riku Seiki,[a] Akito Fujisawa,[a] Akhmad Fadel Fadilla,[a] Fangda Jia,[b] Shin-ichi Ohkoshi [iD] *[b] and Hiroko Tokoro [iD] *[a]

This study reports a simple method for synthesizing λ-Ti₃O₅ through hydrogen reduction calcination using titanium chloride as the starting material. Upon applying 300 MPa pressure, λ-Ti₃O₅ transitions to β-Ti₃O₅ as a pressure-induced phase transformation. The β-Ti₃O₅ produced under pressure reverts to λ-Ti₃O₅ at 462 K upon heating, accumulating 7.78 kJ mol⁻¹ of heat energy. An investigation of the influence of the crystalline size on the threshold pressure required for the phase transition and the values of transition enthalpy of the transition between λ-Ti₃O₅ and β-Ti₃O₅ reveals that larger crystalline sizes correlate with lower threshold pressures and higher transition enthalpies. Understanding the interplay between the crystalline size of λ-Ti₃O₅ and its heat storage properties is crucial for designing phase transition materials tailored to specific heat storage requirements. This research paves the way for the development of more efficient heat storage materials, potentially impacting various industrial applications and energy conservation methods.

Introduction

In recent years, the intensifying issues of climate change and environmental deterioration have emerged as prominent global concerns. Advancing technological innovation is imperative to safeguard the Earth and ensure its preservation for future generations.[1–8] To this end, energy reuse technology—a critical component of energy conservation—has garnered special attention, especially the recovery of waste heat energy. Currently, approximately 40% of the energy obtained from sources such as oil, gas, and coal is emitted as waste heat into the atmosphere. Note that about 80% of this waste heat is < 200 °C (473 K).[9] The development of high-performance thermal storage materials, capable of capturing and transforming sub-200 °C waste heat into usable thermal energy, could significantly mitigate these challenges. Established thermal storage materials include sensible heat storage materials, such as bricks and concrete, and latent heat storage materials, such as water, paraffin, and polyethylene glycol, which utilize solid–liquid phase transitions.[2,10–17] Generally,

thermal storage materials release stored heat energy gradually over time. However, materials that can store heat for extended periods and release it on demand are promising for various practical applications.

Recently, we developed a pressure-responsive thermal storage material that discharges stored heat when subjected to external pressure.[18,19] This material—λ-phase trititanium pentoxide (λ-Ti₃O₅)—is a metastable phase present only in nanoscale materials and not in bulk forms.[18,20] Furthermore, λ-Ti₃O₅ undergoes a reversible phase transition with beta-phase trititanium pentoxide (β-Ti₃O₅) under external stimuli such as light, pressure, or temperature.[18–21] Moreover, λ-Ti₃O₅ is an environmentally friendly material purely composed of titanium and oxygen.[18–22] To effectively use this material, scalable synthesis methods for mass production and strategies for enhancing thermal storage properties are crucial. Accordingly, various synthesis techniques for λ-Ti₃O₅ have been explored. One method involves nanocrystalline λ-Ti₃O₅ synthesis through calcination reduction of TiO₂ nanoparticles in a hydrogen atmosphere.[18,20–25] Another approach uses titanium chloride as the Ti source, employing the sol–gel process to produce λ-Ti₃O₅ nanoparticles within a silica matrix.[20,26–28] Additionally, carbon thermal reduction,[29–32] electrochemical methods,[33,34] and pulse laser deposition (PLD)[35,36] are other notable synthesis methods.

In this research, we detail a method for synthesizing λ-Ti₃O₅ through hydrogen reduction calcination of a precursor, utilizing titanium(IV) chloride as the starting material. This technique enables the efficient production of λ-Ti₃O₅ without employing

[a] Department of Materials Science, Institute of Pure and Applied Sciences, University of Tsukuba, 1-1-1 Tennodai, Tsukuba, Ibaraki 305-8573, Japan. E-mail: tokoro@ims.tsukuba.ac.jp

[b] Department of Chemistry, School of Science, The University of Tokyo, 7-3-1 Hongo, Bunkyo-ku, Tokyo 113-0033, Japan. E-mail: ohkoshi@chem.s.u-tokyo.ac.jp

† Electronic supplementary information (ESI) available: SEM image, PXRD patterns, Rietveld analyses, crystallographic data, magnetic properties, details of parameters in theoretical calculations, calculated fraction *versus* pressure curves, and relationship between ΔH_{trans}, ΔS and P_{th}. See DOI: https://doi.org/10.1039/d3ma01162c
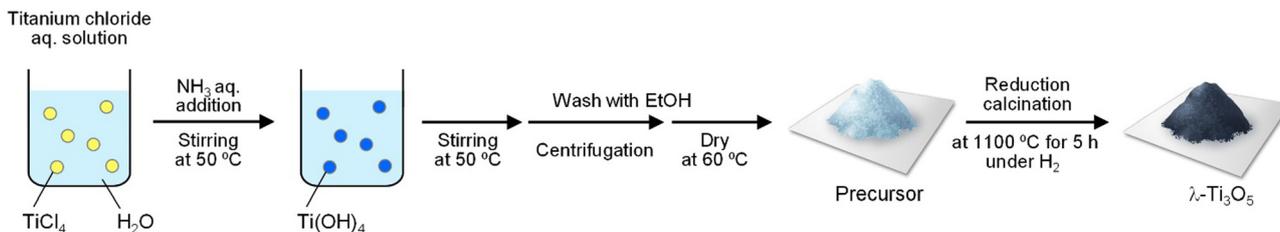
Fig. 1 Synthesis of λ-Ti₃O₅ using titanium(ɪᴠ) chloride as the starting material. Schematic of the synthesis used to prepare the precursor and the calcination procedure.

matrices such as silica. At a pressure of 300 MPa, λ-Ti₃O₅ undergoes a pressure-induced phase transformation to β-Ti₃O₅. During the reverse transition from β-Ti₃O₅ to λ-Ti₃O₅ upon heating, the material stores 7.78 kJ mol^{-1} of heat energy at 462 K. We investigated the relationship between the crystalline size of λ-Ti₃O₅ and the threshold pressure for pressure-induced phase transition and the transition enthalpy values between λ-Ti₃O₅ and β-Ti₃O₅, demonstrating the correlation between crystalline size and heat storage capabilities.

Experimental

Material synthesis

A mixture solution of 420 mL of H_2O, 1.40 mL of $TiCl_4$ (Wako), and 9.6 mL of NH_3 (25 wt%, Wako, ammonia solution) was prepared in a 1-L container. The solution was stirred for 20 h at 50 °C in an oil bath to produce $Ti(OH)_4$ precipitates. These precipitates were separated *via* centrifugation, washed with ethanol, and dried at 60 °C for 24 h (Fig. 1) (eqn (1)).

$$TiCl_4 + 4H_2O + 4NH_3 \rightarrow Ti(OH)_4 + 4NH_4Cl \qquad (1)$$
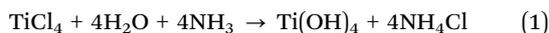
The resulting precipitate underwent calcination under a hydrogen flow rate of 0.5 dm³ min^{-1} at 1100 °C for 5 h, forming a black powder sample (eqn (2)).

$$3Ti(OH)_4 + H_2 \rightarrow Ti_3O_5 + 7H_2O \qquad (2)$$
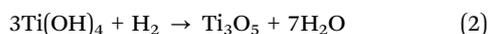
Measurements

Elemental analysis was conducted *via* X-ray fluorescence (XRF) spectroscopy using the Rigaku ZSX Primus IV. The morphology of the synthesiz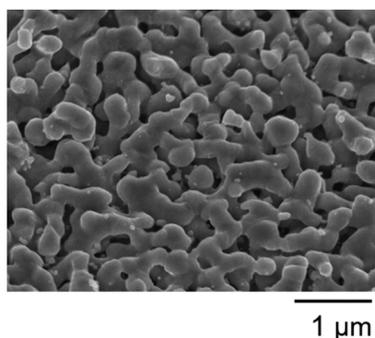ed samples was examined using scanning electron microscopy (SEM) (JSM-7500FA), manufactured by JEOL. Powder X-ray diffraction (PXRD) patterns were obtained using a Rigaku Ultima IV instrument with Cu–Kα radiation ($\lambda = 1.5418$ Å). Rietveld analyses of the PXRD patterns were performed using Rigaku PDXL software. The heat absorption during the phase transition from β-Ti₃O₅ to λ-Ti₃O₅ was measured using a Rigaku differential scanning calorimetry (DSC) Thermo plus EVO2, with liquid nitrogen (N_2) as the cooling agent. Magnetic measurements were conducted using a Quantum Design MPMS superconducting quantum interference device magnetometer.

Results and discussion

Material

According to the XRF measurements, the composition of the synthesized black powder was $Ti_{3.00(3)}O_{5.00(3)}$ (calculated: Ti: 64.22; O: 35.78 wt%; Observed: Ti: 64.53; O: 35.47 wt%). Fig. 2 presents an SEM image of the sample. The sample displayed a flake-like morphology with an average width of 299 ± 54 nm (Fig. S1, ESI†). The PXRD and Rietveld analysis confirmed the samples as monoclinic λ-Ti₃O₅ with the space group $C2/m$ (lattice parameters: $a = 9.8332(2)$ Å, $b = 3.78568(7)$ Å, $c = 9.9688(2)$ Å, $\beta = 91.2589(14)°$), and the crystalline size was estimated to be 57 ± 0.3 nm (Fig. 3 and Fig. S2 and Table S1, ESI†). In other words, this sample was an aggregate with a flake-like structure, approximately 300 nm in width, composed of crystallites of about 57 nm.

In the magnetic susceptibility (χ) *versus* temperature (T) curve, λ-Ti₃O₅ displayed a χ-value of approximately 2×10^{-4} emu per Ti atom over the entire temperature range (Fig. S3, ESI†). This aligns with prior findings identifying λ-Ti₃O₅ as a Pauli paramagnet, stable across the temperature spectrum. The gradual decrease in χ value below 150 K is attributed to the spin–orbit interaction of Ti^{3+} ions. The abrupt increase in magnetic susceptibility below 40 K is possibly because of Curie paramagnetism resulting from minor defects in the sample.[20]

Pressure-induced phase transition

We investigated the effects of pressure on the crystal structure. The pellets subjected to varying uniaxial pressures were analyzed, and their PXRD patterns were measured. As demonstrated in Fig. 3 and Fig. S4–S13 and Tables S2–S11 (ESI†), increasing pressure led to a decrease in the λ-Ti₃O₅ fraction and

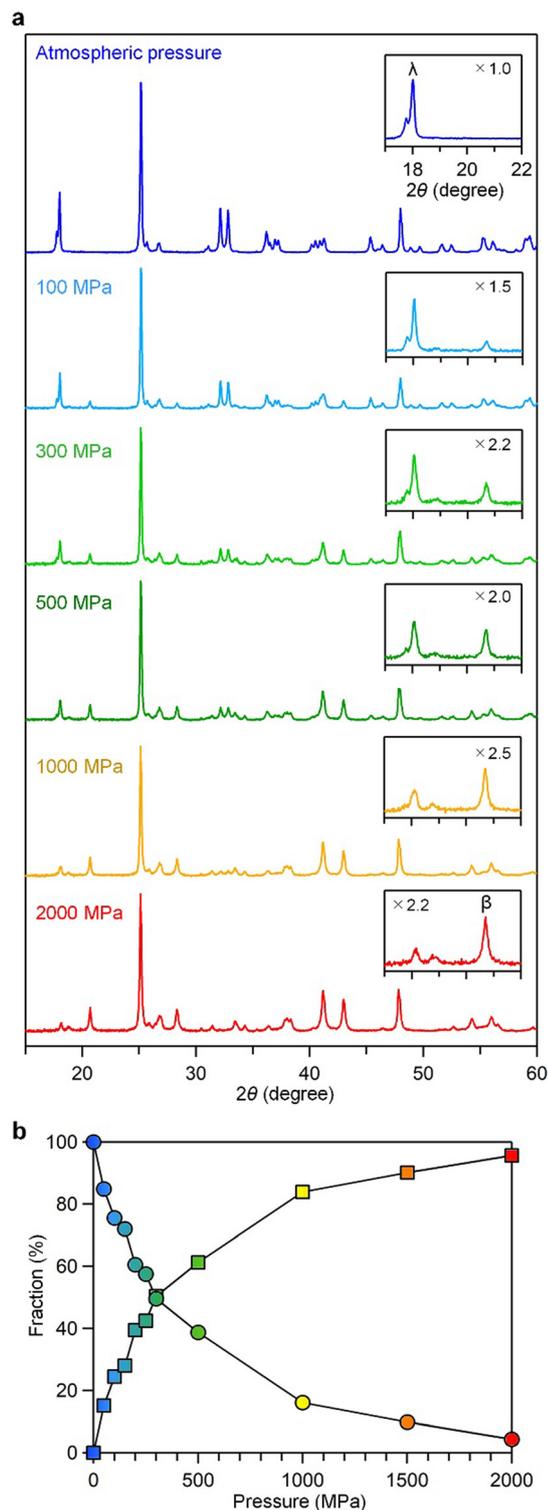**Fig. 2** SEM image of the obtained λ-Ti₃O₅ particles.

a

b

Fig. 3 (a) PXRD patterns without applying pressure (blue), and after releasing pressures of 100 MPa (light blue), 300 MPa (light green), 500 MPa (green), 1000 MPa (orange), and 2000 MPa (red). (b) Phase fraction of λ-Ti$_3$O$_5$ (circle) and β-Ti$_3$O$_5$ (square) as a function of applied pressure.

an increase in β-Ti$_3$O$_5$. The threshold pressure value (P_{th}) for converting 50% of λ-Ti$_3$O$_5$ to β-Ti$_3$O$_5$ was approximately 300 MPa (Fig. 3b). The crystal structure of β-Ti$_3$O$_5$ formed after

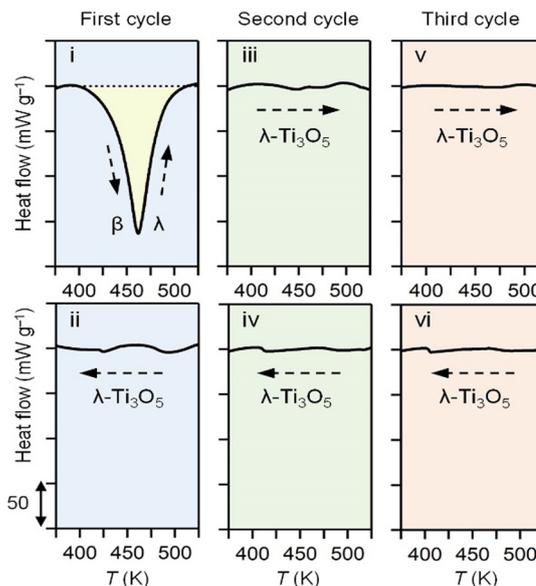**Fig. 4** DSC measurements for pressure-produced β-Ti$_3$O$_5$ by heating (i) and cooling (ii). Second cycle of heating (iii) and cooling (iv), and third cycle of heating (v) and cooling (vi).

a 2000 MPa pressure was monoclinic with lattice parameters a = 9.7540(6) Å, b = 3.7993(2) Å, c = 9.4428(6) Å, $β$ = 91.528(3)° (space group $C2/m$) (Fig. S13 and Table S11, ESI†).

Accumulated heat energy

To investigate the heat energy accumulated during the phase transition from β-Ti$_3$O$_5$ to λ-Ti$_3$O$_5$, DSC measurements were conducted using β-Ti$_3$O$_5$ samples after applying a pressure of 300 MPa and releasing the pressure (Fig. 4). The transition from β-Ti$_3$O$_5$ to λ-Ti$_3$O$_5$ occurred at 462 K, and the observed transition enthalpy (ΔH_{trans}) during this temperature-induced phase transition was 7.78 ± 0.26 kJ mol^{-1} (Fig. 4, i). Subsequent cooling of the sample during DSC measurements revealed no peaks (Fig. 4, ii), indicating that the heat energy accumulated during the β-Ti$_3$O$_5$ to λ-Ti$_3$O$_5$ phase transition was not released upon cooling. Moreover, once transformed into λ-Ti$_3$O$_5$, the sample exhibited no peaks in repeated heating and cooling cycles (Fig. 4, iii–vi), highlighting the stability of λ-Ti$_3$O$_5$.

Thermodynamic interpretation of the threshold pressure

The threshold pressure for the phase transition from λ-Ti$_3$O$_5$ to β-Ti$_3$O$_5$ was analyzed using the Slichter and Drickamer mean-field thermodynamic model (SD model).[18,20,37] In this model, the Gibbs free energy (G) is expressed as

$$G = x\Delta H + \gamma x(1 - x) + T\{R[x \ln x + (1 - x)\ln(1 - x)] - x\Delta S\},$$

where x represents the fraction of charge delocalization units corresponding to λ-Ti$_3$O$_5$; ΔH denotes the transition enthalpy, and ΔS indicates the transition entropy. γ represents the interaction parameter between the λ-Ti$_3$O$_5$ and β-Ti$_3$O$_5$ phases, and R denotes the gas constant. The origin of the energy is set to be the Gibbs free energy of β-Ti$_3$O$_5$ (x = 0). Using the
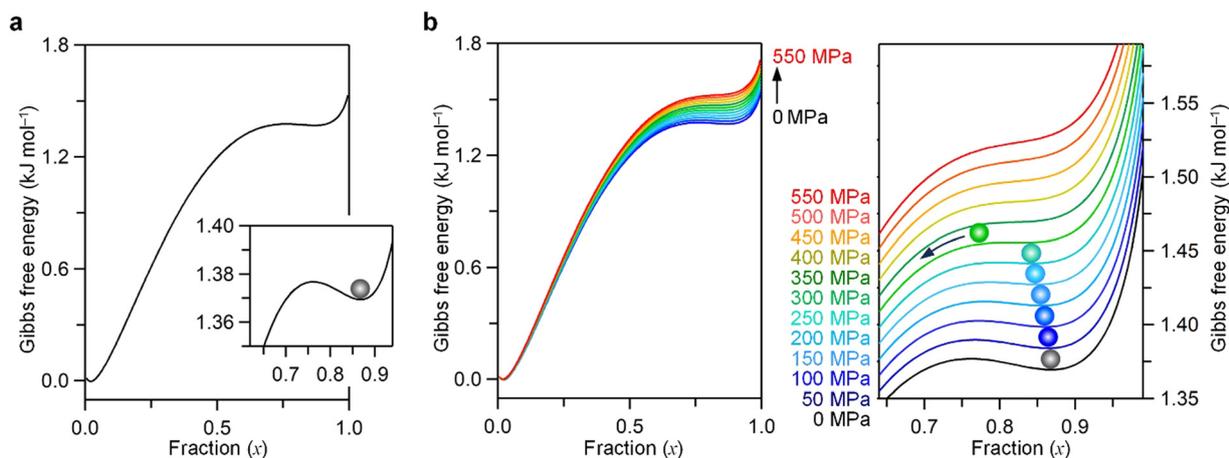
Fig. 5 (a) Gibbs free energy *versus* fraction curve at 300 K for pressure of 0. Ball indicates the thermal population. λ-Ti$_3$O$_5$ cannot transit to β-Ti$_3$O$_5$ since the energy barrier exists. (b) Pressure dependence of Gibbs free energy *versus* fraction curves. λ-Ti$_3$O$_5$ transits to β-Ti$_3$O$_5$ by applying pressure because the energy barrier disappears.

experimentally observed ΔH_{trans} value (7.78 kJ mol^{-1}) and ΔS_{trans} value (21.0 J K^{-1} mol^{-1}) from the DSC measurements, the Gibbs free energy curve for the bistable state was calculated at 300 K, as depicted in Fig. 5a (S6, ESI†). This equilibrium state reveals an energy barrier between λ-Ti$_3$O$_5$ and β-Ti$_3$O$_5$, suggesting that λ-Ti$_3$O$_5$, synthesized *via* high-temperature calcination and cooled to room temperature, does not spontaneously convert to β-Ti$_3$O$_5$. Conversely, applying pressure at 300 K reduces this energy barrier between λ-Ti$_3$O$_5$ and β-Ti$_3$O$_5$ dec (Fig. 5b), which vanishes at 300 MPa. The pressure at which this energy barrier disappears is identified as the theoretical threshold pressure.

Relationship between crystalline size, ΔH_{trans} and P_{th}

Subsequently, we investigated the relationship between crystalline size, ΔH_{trans} and P_{th}, wherein crystalline size was estimated as 57 nm with a spherical shape, ΔH_{trans} is obtained as 7.78 kJ mol^{-1}, and P_{th} was experimentally observed at 300 MPa. In previous reports, various values of P_{th} with different crystalline sizes have been reported. For instance, the P_{th} for flake-shaped λ-Ti$_3$O$_5$ (crystal size: 25 nm, cubic shape) was 400 MPa,[20] whereas the P_{th} for stripe-shaped λ-Ti$_3$O$_5$ (crystal size: 200 × 30 nm, rectangular prism shape) was 60 MPa.[18] The value of P_{th} for block-shaped λ-

Ti$_3$O$_5$ (crystal size: 400 nm, cubic shape) was 7 MPa.[24] Furthermore, λ-Ti$_3$O$_5$ synthesized using a block copolymer (crystal size: 54 nm, spherical shape, S5, ESI†) exhibited a P_{th} of 300 MPa.[23] The relationship between the P_{th} values and the crystalline size (crystalline volume) of λ-Ti$_3$O$_5$ is plotted in Fig. 6a, exhibiting a clear size dependency of P_{th}, *i.e.*, P_{th} decreases as the crystalline size increases.

This trend led us to consider that the P_{th} diminishes with increasing crystalline size. As the crystalline size decreases, the ratio of surface atoms to total atoms in the crystal ($\alpha = N_{\text{surface}}/N_{\text{total}}$) increases, enhancing the significance of surface energy in the Gibbs free energy of the crystal. Fig. 6b illustrates the inverse relationship between ΔH_{trans} and α: a smaller α corresponds to a larger ΔH_{trans}, and *vice versa*. Similarly, Fig. 6c demonstrates the direct relationship between P_{th} and α: a larger α results in a higher P_{th}. These observations suggest that as the crystalline size reduces, α increases, leading to a heightened surface energy contribution to the Gibbs free energy, consequently reducing ΔH_{trans}. A decrease in ΔH_{trans} consequently correlates with an increase in P_{th} (Fig. 6d). Employing the Slichter and Drickamer model to manipulate ΔH values, we observed that a smaller ΔH aligns with a higher P_{th}, whereas a larger ΔH associates with a lower P_{th} (Fig. S15, ESI†). Surface

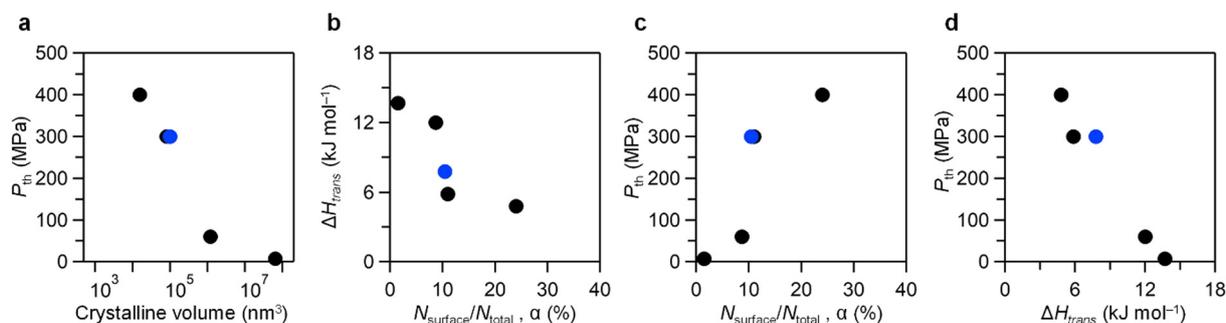**Fig. 6** (a) P_{th} *versus* crystalline volume plot, (b) ΔH_{trans} *versus* $N_{\text{surface}}/N_{\text{total}}$ plot, (c) P_{th} *versus* $N_{\text{surface}}/N_{\text{total}}$ plot, and (d) P_{th} *versus* ΔH_{trans} plot. Black circles indicate previously reported data,[18,20,23,24] whereas blue circles indicate data from the present study.

effects influence not only enthalpy but also entropy. Fig. S16 (ESI†) shows the ΔS versus ΔH_{trans} plot. As ΔH_{trans} increases, ΔS also increases. Fig. S17 (ESI†) shows the P_{th} versus ΔS plot. The influence of ΔS on P_{th} suggests a similar trend to that of ΔH_{trans}.

Conclusions

In this research, we introduced a simple synthesis technique for producing $\lambda\text{-Ti}_3O_5$ without the use of matrices such as silica. This method involves hydrogen reduction calcination of a precursor derived from titanium(IV) chloride. The resultant $\lambda\text{-Ti}_3O_5$ had a crystalline size of ~ 57 nm, and the threshold pressure required for its phase transition from $\lambda\text{-Ti}_3O_5$ to $\beta\text{-Ti}_3O_5$ was ca. 300 MPa. The transition from $\beta\text{-Ti}_3O_5$ -Ti$_3O_5$ occurred at 462 K, leading to the accumulation of 7.78 kJ mol^{-1} of heat energy.

The examination of the relationship between crystalline size and the threshold pressure and transition enthalpy values between $\lambda\text{-Ti}_3O_5$ and $\beta\text{-Ti}_3O_5$ demonstrated that a reduction in crystalline size and an increase in the proportion of surface atoms intensified the influence of surface energy on the Gibbs free energy. This decreases the transition enthalpy and consequently increases the threshold pressure. Understanding the relationship between the crystalline size and heat storage properties is essential for developing effective heat storage materials in contemporary society.

The synthesis method utilizing titanium(IV) chloride as the starting material provides an economical and efficient route to produce $\lambda\text{-Ti}_3O_5$, suitable for large-scale manufacturing. Given the broad availability of metal chlorides for various metals, this approach is a viable candidate for preparing metal-substituted $\lambda\text{-Ti}_3O_5$. Although certain metal-substituted $\lambda\text{-Ti}_3O_5$ has been previously reported,[38–45] those methods typically involve calcination or melting of titanium oxide particles with different metals. The synthesis technique presented in this study offers potential for homogeneous doping using diverse metal chlorides as starting materials to prepare the precursor, enabling greater versatility in the synthesis of metal-substituted $\lambda\text{-Ti}_3O_5$.

Author contributions

T. K. and A. F. F. conducted sample synthesis, characterization, and data analysis and contributed to the preparation of the manuscript. R. S. and A. F. performed sample synthesis, characterization, and DSC measurements. F. J. contributed to sample synthesis and characterization. S. O. contributed to data analysis and coordinated this study. H. T. designed and coordinated the study, contributed to all measurements, performed calculations, and wrote the manuscript. All authors participated in the discussion and editing of the manuscript.

Conflicts of interest

The authors declare no competing financial interests.

Acknowledgements

References

1 D. B. Gingerich and M. S. Mauter, Quantity, Quality, and Availability of Waste Heat from United States Thermal Power Generation, Environ. Sci. Technol., 2015, 49, 8297–8306.

2 I. Gur, K. Sawyer and R. Prasher, Searching for a Better Thermal Battery, Science, 2012, 335, 1454–1455.

3 E. Cartlidge, Saving for a rainy day, Science, 2011, 334, 922–924.

4 D. Lindley, The energy should always work twice, Nature, 2009, 458, 138–141.

5 A. Sharma, V. V. Tyagi, C. R. Chen and D. Buddhi, Review on thermal energy storage with phase change materials and applications, Renewable Sustainable Energy Rev., 2009, 13, 318–345.

6 C. W. King, A. S. Holman and M. E. Webber, Thirst for energy, Nat. Geosci., 2008, 1, 283–286.

7 D. Butler, Solar power: California's latest gold rush, Nature, 2007, 450, 768–769.

8 G. W. Crabtree and N. S. Lewis, Solar energy conversion, Phys. Today, 2007, 60, 37–42.

9 A. Kondo, NEDO, presented in part the 10th German-Japanese Environment and Energy Dialogue Forum, Tokyo, 2019 **https://www.nedo.go.jp/content/100899759.pdf**.

10 Q. Cao and P. Liu, Hyperbranched polyurethane as novel solid-solid phase change material for thermal energy storage, Eur. Polym. J., 2006, 42, 2931–2939.

11 K. S. Al-Jabri, A. W. Hago, A. S. Al-Nuaimi and A. H. Al-Saidy, Concrete blocks for thermal insulation in hot climate, Cem. Concr. Res., 2005, 35, 1472–1479.

12 M. M. Farid, A. M. Khudhair, S. A. K. Razack and S. Al-Hallaj, A review on phase change energy storage: materials and applications, Energy Convers. Manage., 2004, 45, 1597–1615.

13 W. Li, D. Zhang, T. Zhang, T. Wang, D. Ruan, D. Xing and H. Li, Study of solid–solid phase change of $(n\text{-}C_nH_{2n+1}NH_3)_2MCl_4$ for thermal energy storage, Thermochim. Acta, 1999, 326, 183–186.

14 M. Barrio, D. O. López, J. L. Tamarit, P. Negrier and Y. Haget, Molecular interactions and packing in molecular alloys between nonisomorphous plastic phases, J. Solid State Chem., 1996, 124, 29–38.

15 D. K. Benson, R. W. Burrows and J. D. Webb, Solid state phase transitions in pentaerythritol and related polyhydric alcohols, Sol. Energy Mater., 1986, 13, 133–152.

16 V. Busico, C. Carfagna, V. Salerno, M. Vacatello and F. Fittipaldi, The layer perovskites as thermal energy storage systems, *Sol. Energy*, 1980, **24**, 575–579.

17 M. K. Nahas and F. H. Constable, Thermal conductivity of mud brick, *Nature*, 1938, **142**, 837.

18 H. Tokoro, M. Yoshikiyo, K. Imoto, A. Namai, T. Nasu, K. Nakagawa, N. Ozaki, F. Hakoe, K. Tanaka, K. Chiba, R. Makiura, K. Prassides and S. Ohkoshi, External stimulation-controllable heat-storage ceramics, *Nat. Commun.*, 2015, **6**, 7037.

19 S. Ohkoshi, M. Yoshikiyo, J. MacDougall, Y. Ikeda and H. Tokoro, Long-term heat-storage materials based on λ-Ti$_3$O$_5$ for green transformation (GX), *Chem. Commun.*, 2023, **59**, 7875–7886.

20 S. Ohkoshi, Y. Tsunobuchi, T. Matsuda, K. Hashimoto, A. Namai, F. Hakoe and H. Tokoro, Synthesis of a metal oxide with a room-temperature photoreversible phase transition, *Nat. Chem.*, 2010, **2**, 539–545.

21 C. Mariette, M. Lorenc, H. Cailleau, E. Collet, L. Guérin, A. Volte, E. Trzop, R. Bertoni, X. Dong, B. Lépine, O. Hernandez, E. Janod, L. Cario, V. Ta Phuoc, S. Ohkoshi, H. Tokoro, L. Patthey, A. Babic, I. Usov, D. Ozerov, L. Sala, S. Ebner, P. Böhler, A. Keller, A. Oggenfuss, T. Zmofing, S. Redford, S. Vetter, R. Follath, P. Juranic, A. Schreiber, P. Beaud, V. Esposito, Y. Deng, G. Ingold, M. Chergui, G. F. Mancini, R. Mankowsky, C. Svetina, S. Zerdane, A. Mozzanica, A. Bosak, M. Wulff, M. Levantino, H. Lemke and M. Cammarata, Strain wave pathway to semiconductor-to-metal transition revealed by time-resolved X-ray powder diffraction, *Nat. Commun.*, 2021, **12**, 1239.

22 B. Yang, Z. Zhang, P. Liu, X. Fu, J. Wang, Y. Cao, R. Tang, X. Du, W. Chen, S. Li, H. Yan, Z. Li, X. Zhao, G. Qin, X.-Q. Chen and L. Zuo, Flatband λ-Ti$_3$O$_5$ towards extraordinary solar steam generation, *Nature*, 2023, **622**, 499–506.

23 Y. Araki, S. Ohkoshi and H. Tokoro, Synthesis of λ-Ti$_3$O$_5$ nanocrystals using a block copolymer, *Mater. Today Energy*, 2020, **18**, 100525.

24 S. Ohkoshi, H. Tokoro, K. Nakagawa, M. Yoshikiyo, F. Jia and A. Namai, Low-pressure-responsive heat-storage ceramics for automobiles, *Sci. Rep.*, 2019, **9**, 13203.

25 F. Hakoe, H. Tokoro and S. Ohkoshi, Dielectric and optical constants of λ-Ti$_3$O$_5$ film measured by spectroscopic ellipsometry, *Mater. Lett.*, 2017, **188**, 8–12.

26 G. Batdembere, Y. Ganchimeg, M. Enkhtuul, O Enkhtsolmon, G. Munkhsaikhan and D. Otgonbayar, Synthesis and Characterization of Nanosized Ti$_3$O$_5$ Crystals under Inert Gas Flow, *Nano Hybrids Composites*, 2022, **39**, 73–79.

27 Y. Cai, Q. Shi, M. Wang, X. Lv, Y. Cheng and W. Huang, Synthesis of nanoscale lambda-Ti$_3$O$_5$ via a PEG assisted sol-gel method, *J. Alloys Compd.*, 2020, **848**, 156585.

28 T. Nasu, H. Tokoro, K. Tanaka, F. Hakoe, A. Namai and S. Ohkoshi, Sol–gel synthesis of nanosized λ-Ti$_3$O$_5$ crystals, *Mater. Sci. Eng.*, 2014, **54**, 012008.

29 Q. Shi, G. Chai, W. Huang, Y. Shi, B. Huang, D. Wei, J. Qi, F. Su, W. Xu and T. Lu, Fabrication of nanocrystalline λ-Ti$_3$O$_5$ with tunable terahertz wave transmission properties across a temperature induced phase transition, *J. Mater. Chem. C*, 2016, **4**, 10279–10285.

30 X. Zhang, W. Liu, H. Yu, X. Zhong, L. Wang, A. Singh and Y. Lin, Preparation and oxygen sensing properties of Ti$_3$O$_5$ submicron rods, *Micro Nano Lett.*, 2016, **11**, 811–813.

31 D. Wei, W. Huang, Q. Shi, T. Lu and B. Huang, Effect of coating layers on nano-TiO$_2$ particles on the preparation of nanocrystalline λ-Ti$_3$O$_5$ by carbothermal reduction, *J. Mater. Sci.: Mater. Electron.*, 2016, **27**, 4216–4222.

32 G. Chai, W. Huang, Q. Shi, S. Zheng and D. Wei, Preparation and characterization of λ-Ti$_3$O$_5$ by carbothermal reduction of TiO$_2$, *J. Alloys Compd.*, 2015, **621**, 404–410.

33 Z. Ertekin, N. Ö. Pekmez and K. Pekmez, One-step electrochemical deposition of thin film titanium suboxide in basic titanyl sulfate solution at room temperature, *J. Solid State Electrochem.*, 2020, **24**, 975–986.

34 Z. Ertekin, U. Tamer and K. Pekmez, Cathodic electrochemical deposition of Magnéli phases Ti$_n$O$_{2n-1}$ thin films at different temperatures in acetonitrile solution, *Electrochim. Acta*, 2015, **163**, 77–81.

35 K. Yoshimatsu and H. Kumigashira, Direct Synthesis of Metastable λ-Phase Ti$_3$O$_5$ Films on LaAlO$_3$ (110) Substrates at High Temperatures, *Cryst. Growth Des.*, 2022, **22**, 703–710.

36 H. Chen, Y. Hirose, K. Nakagawa, K. Imoto, S. Ohkoshi and T. Hasegawa, Non-metallic electrical transport properties of a metastable λ-Ti$_3$O$_5$ thin film epitaxially stabilized on a pseudobrookite seed layer, *Appl. Phys. Lett.*, 2020, **116**, 201904.

37 C. P. Slichter and H. G. Drickamer, Pressure-induced electronic changes in compounds of iron, *J. Chem. Phys.*, 1972, **56**, 2142–2160.

38 F. Jia, M. Yoshikiyo, R. Makuta, K. Kawakami, H. Tokoro and S. Ohkoshi, Observation of a Pressure Effect on an Al-substituted λ-Ti$_3$O$_5$ Heat-storage Material, *Chem. Lett.*, 2023, **52**, 748–751.

39 S. Jütten and T. Bredow, Doping Effect on the Electronic Structure and Heat-Storage Properties of Ti$_3$O$_5$, *J. Phys. Chem. C*, 2023, **127**, 10445–10452.

40 S. Ohkoshi, F. Jia, M. Yoshikiyo, K. Imoto, H. Tokoro, K. Nakagawa, Y. Maeno, A. Namai, R. Harada, K. Hattori, K. Kojima, K. Sugiura and T. Suganuma, Pressure effect on long-term heat storage ceramics based on Mg-substituted λ-Ti$_3$O$_5$, *Mater. Adv.*, 2022, **3**, 4824–4830.

41 X. Fu, W. Chen, X. Hao, Z. Zhang, R. Tang, B. Yang, X. Zhao and L. Zuo, Preparing high purity λ-Ti$_3$O$_5$ and Li/λ-Ti$_3$O$_5$ as high-performance electromagnetic wave absorbers, *J. Mater. Chem. C*, 2021, **9**, 7976–7981.

42 Y. Nakamura, Y. Sakai, M. Azuma and S. Ohkoshi, Long-term heat-storage ceramics absorbing thermal energy from hot water, *Sci. Adv.*, 2020, **6**, eaaz5264.

43 M. Wang, W. Huang, Z. Shen, J. Gao, Y. Shi, T. Lu and Q. Shi, Phase evolution and formation of λ phase in Ti$_3$O$_5$ induced by magnesium doping, *J. Alloys Compd.*, 2019, **774**, 1189–1194.

44 R. Takahama, T. Ishii, D. Indo, M. Arizono, C. Terakura, Y. Tokura, N. Takeshita, M. Noda, H. Kuwahara, T. Saiki, T. Katsufuji, R. Kajimoto and T. Okuda, Structural, magnetic, transport, and thermoelectric properties of the pseudobrookite AlTi$_2$O$_5$-Ti$_3$O$_5$ system, *Phys. Rev. Mater.*, 2020, **4**, 074401.

45 Z. Shen, Q. Shi, W. Huang, B. Huang, M. Wang, J. Gao, Y. Shi and T. Lu, Stabilization of microcrystal λ-Ti$_3$O$_5$ at room temperature by aluminum-ion doping, *Appl. Phys. Lett.*, 2017, **111**, 191902.